Supplementary Material

Table of contents

Supplementary Figures

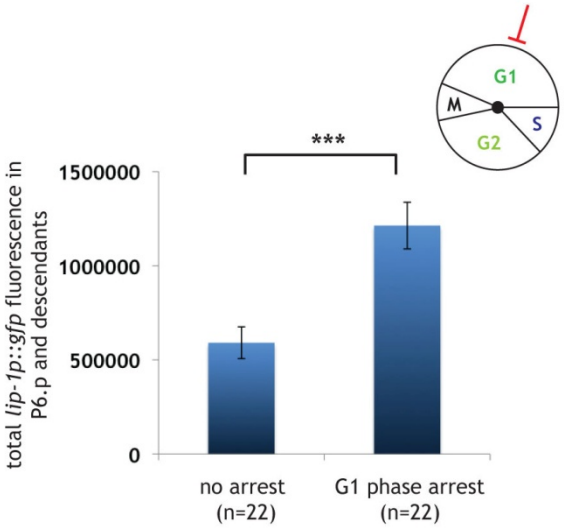

Suppl. Fig. s1. Quantification of *lip-1p::gfp* expression corrected for total area of the nuclei. The possibility that divided cells show lower signal intensities due to a dilution effect can be ruled out because there is a significant difference in the signal intensities corrected for total nuclear area between arrested P6.p versus the P6.px and P6.pxx cells. Error bars indicate the standard errors and asterisks the significance calculated as described in materials and methods.

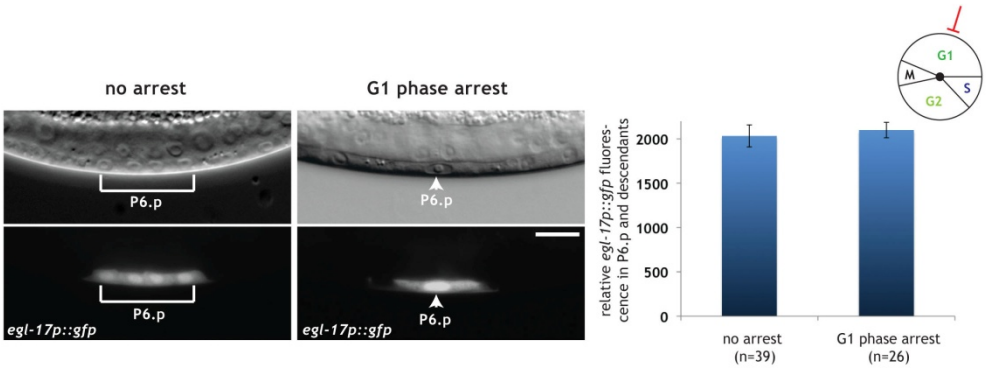

Suppl. Fig. s2. Expression of the 1° cell fate marker *egl-17p::gfp* in the G1 arrested P6.p cell of an *egl-17p::cki-1* transgenic animal at the Pn.pxx stage (arrowheads in the right panels) and in the P6.p descendants of a sibling that had lost the e*gl-17p::cki-1* array (brackets in the left panels). The corresponding Nomarski images are shown on top. The scale bar represents 10 µm. Quantification of *egl-17p::gfp* expression is shown to the right. Error bars indicate the standard errors as described in materials and methods.

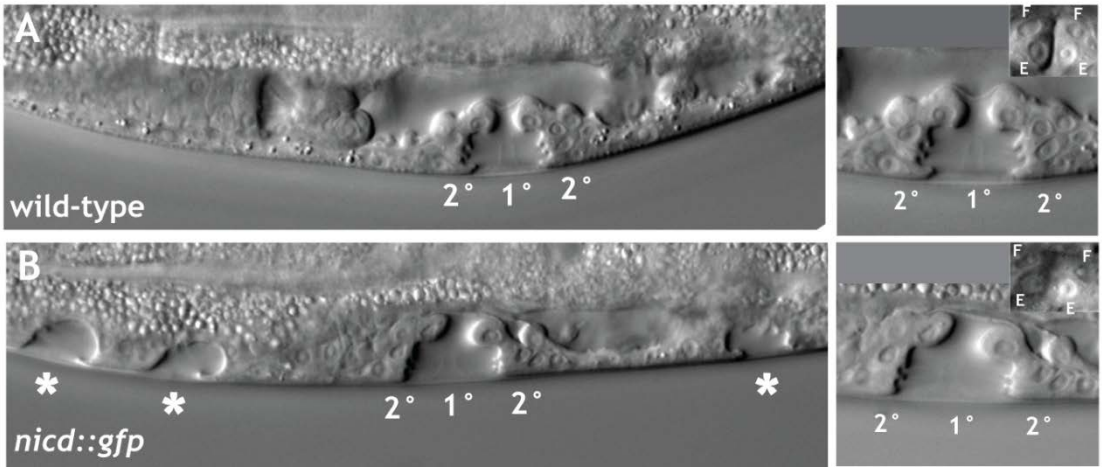

Suppl. Fig. s3. (A) Nomarski images of the vulva in a wild-type and **(B)** *nicd::gfp* L4 larva. Asterisks in the lower panel indicate ectopic inductions in the *nicd::gfp* larva. The right panels both show a higher magnifications of the 2°-1°-2° vulval invagination formed by the P5.p, P6.p and P7.p descendants. The insets show a focal plane, in which the nuclei of four of the eight 1° descendants of P6.p (VulE and VulF) are visible.

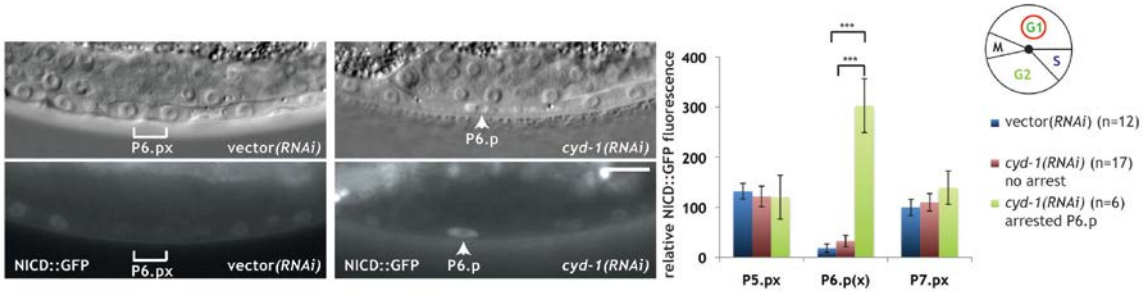

Suppl. Fig. s4. NICD::GFP expression in the G1 arrested P6.p cell of an *cyd-1* RNAi treated animal at the Pn.px stage (arrowheads in the right panels) and in the P6.p descendants of a control animal treated with empty vector RNAi (brackets in the left panels). The corresponding Nomarski images are shown on top. The scale bar is 10 μm. Quantification of NICD::GFP expression is shown to the right. Note that *cyd-1* RNAi per se did not increase NICD::GFP levels (red bars), except for the six strongly affected animals, in which P6.p was arrested (green bar). Error bars and asterisks indicate the standard errors and the significance as described in materials and methods.

Computational model of VPC fate specification based on the cell-cycle

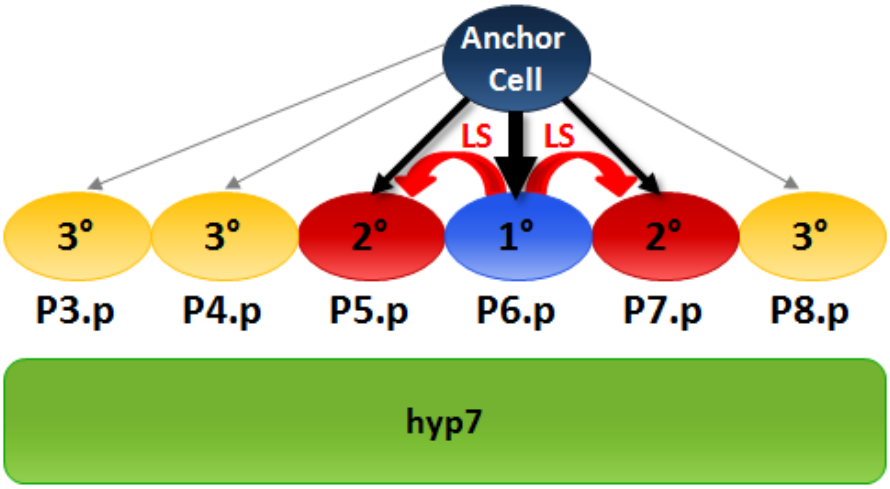

Suppl. Fig. s5. Simplified representation of the *C. elegans* VPC system showing the six VPCs, the anchor cell and the hypodermis (hyp7) with intercellular signals. Colors indicate the cell fates as induced by the anchor cell in wild-type animals.

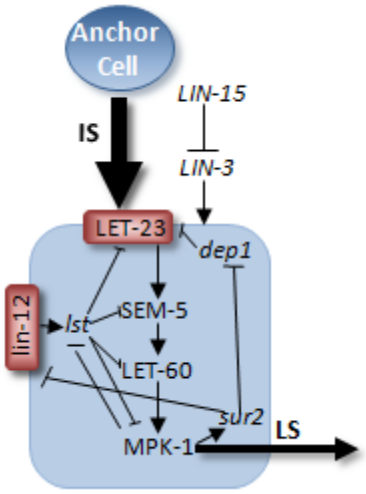

Suppl. Fig. s6. Schematic representation of one VPC and the anchor cell with intra- and extra-cellular components and interactions between components as implemented in the presented model. LS refers to the lateral signal between VPCs and IS represents the inductive signal from the anchor cell to the VPC.

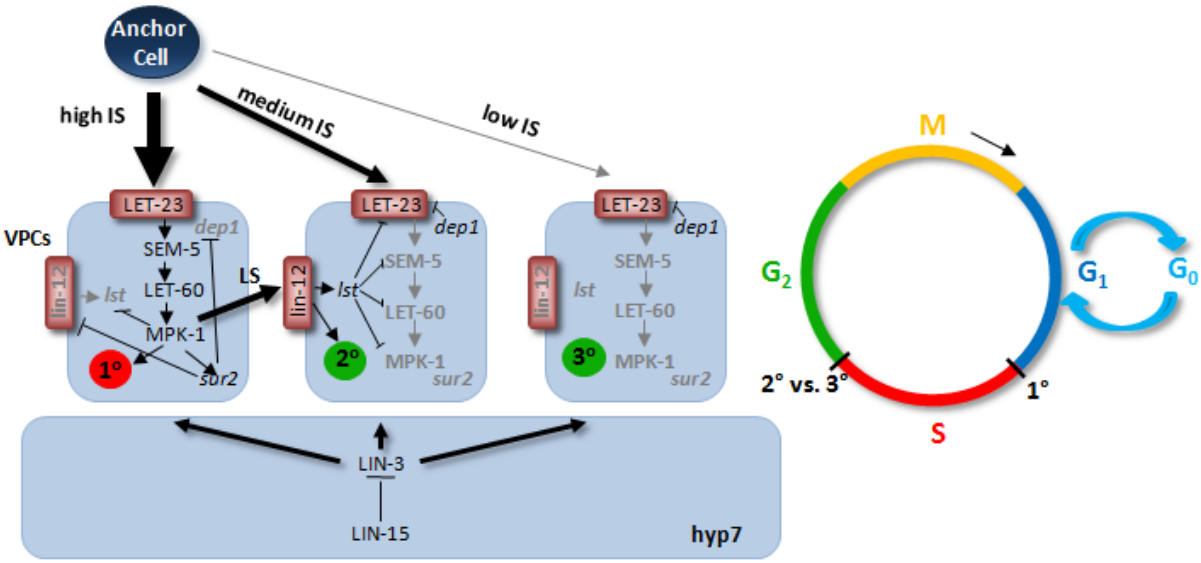

Suppl. Fig. s7. Inclusion of Cell-cycle: Three VPCs, P6.p, P7.p and P8.p (from left), with the components, interactions, fate specifications and their connections to the cell-cycle in a wild-type animal used in the present model. Grey arrows and component names indicate low or medium activation of pathways and components. The timing of cell fate decisions is indicated in the figure of the cell-cycle on the right.

We have updated a previous model of the six vulval precursor cells (VPCs, cells shown in Figure s5) by Fisher and colleagues (2007) according to the current biological understanding. Figure 2 shows a representation of one VPC and its components as represented in our model. Furthermore, we have included the cell-cycle into the model presented here as a timer for certain aspects of the model behavior (see Figure s7). The present model was constructed and analyzed using the formal verification tool NuSMV [1]. The tool allows for the construction of a model with several modules and variables defined within each module. A state of the model system is described by the states of its modules, which are again characterized by the states (values) of their variables. Variables are defined by their initial state and possible transitions to the following states. If a transition takes place and which one that will depend on the current state of the variable and usually also the state of other variables in the same or other modules. A sequence of these states during an execution defines the behavior of the model system.

Our model consists of a main module that comprises an anchor cell module and six copies of a VPC module, as well as a module controlling the initial states of all variables and two modules influencing the timing of the execution. The copies of the VPC module all start from the same initial conditions defined by the genetic background given in the organizer module. However, they receive a different amount of inductive signal depending on their distance from the anchor cell (AC) and each of them runs its individual copy of the same program. This results in a different outcome for each of the VPCs based on the amount of inductive signal received and communications between the VPCs.

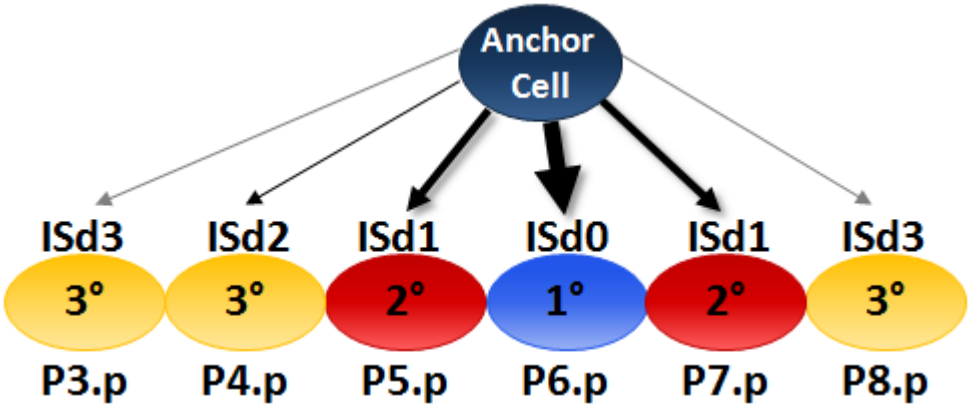

Suppl. Fig. s8. Representation of the six VPCs with the AC and the variables representing their respective inductive signal (ISd0 through ISd3). The AC is located slightly anterior of P6.p.

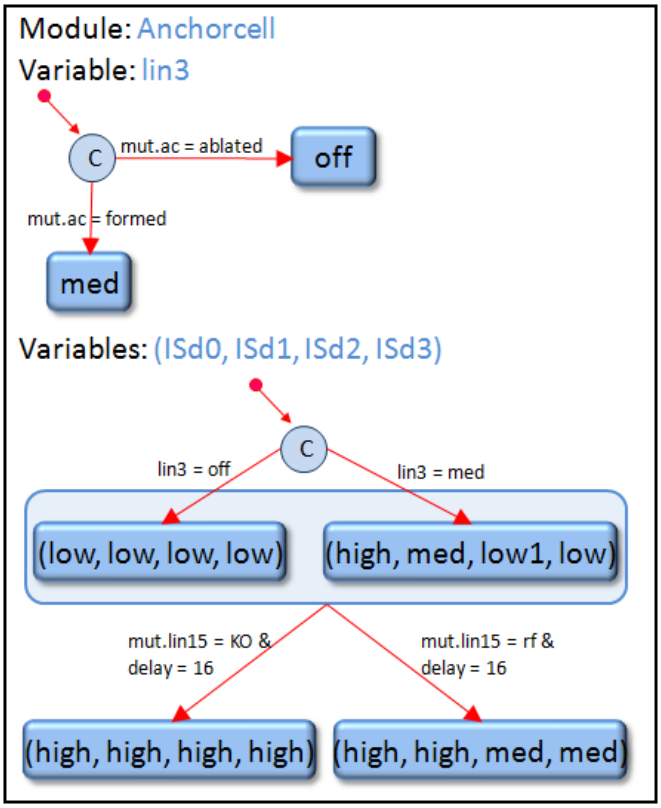

Suppl. Fig. s9. Representation of the state-transitions in the anchor cell module. Blue boxes represent the possible states of the described variables. Red arrows indicate possible transitions. The writing on the arrows indicates the Boolean condition allowing for these transitions. If either of the states in the light blue box is taken, the transitions originating from this box are permitted under the respective conditions. The circled C denotes a condition between two states.

In the following, we explain how the two main functional modules of the presented model, the AC and the VPC modules, are defined and how they work.
The anchor cell module contains a variable indicating if the AC is formed or ablated, a variable indicating the state of lin15 (wild-type (wt), loss of function (lf) or reduction of function (rf)) as well as variables defining the resulting inductive signal

(IS). There are four different variables representing the inductive signal for groups of the VPCs depending on their distance to the AC, which is located opposite P6.p but slightly to its anterior site towards P5.p (Figure s8). With a formed AC, the cell closest to it, P6.p, receives the highest IS (variable ISd0), its neighbors, P5.p and P7.p, receive the next highest signal (variable ISd1), P3.p and P8.p receive the lowest IS (variable ISd3). Because of the special location of the AC, P4.p is closer to the AC than P8.p, so we added a specific IS variable to account for a slightly higher signal than the outer cells (variable ISd2, Figure s8). The overall values of the inductive signal variables depend on the states of the AC and lin15 (see Figure s9). The variable lin15 collectively represents the state of the gene *lin-15* and other synMuv genes in the hypodermis (hyp7). It mediates the inhibition of the LIN-3 EGF signal in hyp7 (see Figure s6). That is, under wild-type conditions *lin-15* is turned on constitutively and the inductive LIN-3 signal is solely dependent on the state of the AC. Reducing *lin-15* function, however, will lead to a higher inductive signal depending on the strength of the *lin-15* mutation (complete loss of function or reduction of function). The model allows for this increase in inductive signal only after a certain delay if the variable lin15 is mutated. Complete loss of function will result in a high inductive signal for all of the VPCs and reduced function of lin15 causes a high inductive signal for both groups of cells closest to the AC and a medium signal for the two groups furthest away (see Figure s9). As can be seen in Figure 5, the initial level of IS is determined solely by the AC state (i.e. it is treated as if lin15 was not mutated) before it increases in this way.

The VPC module contains variables representing the EGFR/RAS/MAPK pathway and the LIN-12 NOTCH lateral signaling pathway, the variables sur2 and dep1 acting downstream of the EGFR/RAS/MAPK pathway as well as variables representing the cell-cycle phase and the fate of the VPC. The functions of the variables and the pathways are described subsequently.

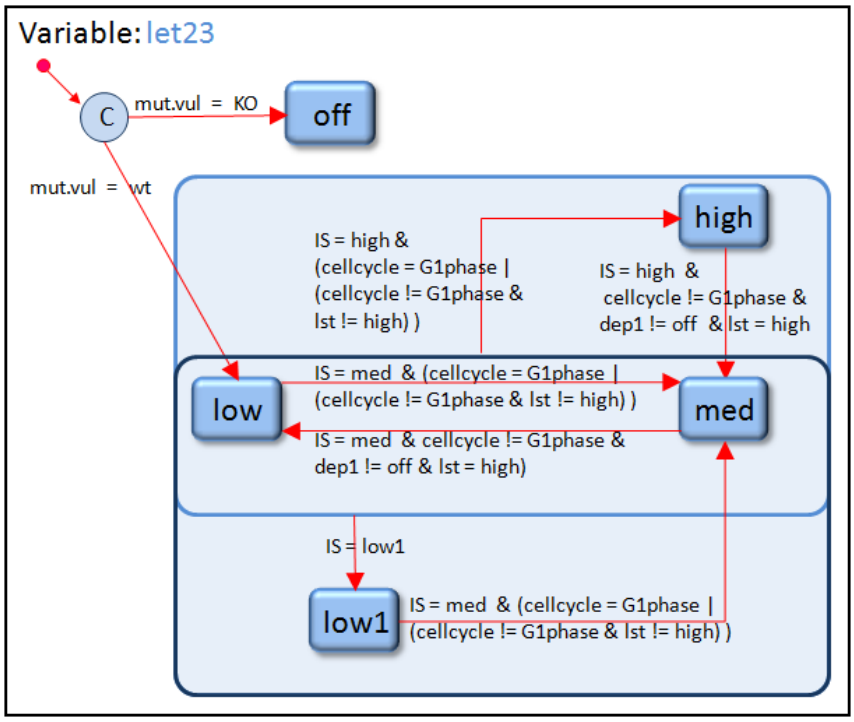

Suppl. Fig. s10. Representation of the state-transitions for the let23 variable. Blue boxes represent the different possible states of the variable. Red arrows indicate possible transitions. The writing on the arrows indicates the Boolean condition allowing for these transitions. If either of the states in one of the light blue boxes is taken, the transitions originating from the respective box are permitted under the stated conditions in addition to the usual transitions between states. The circled C denotes a condition between two states.

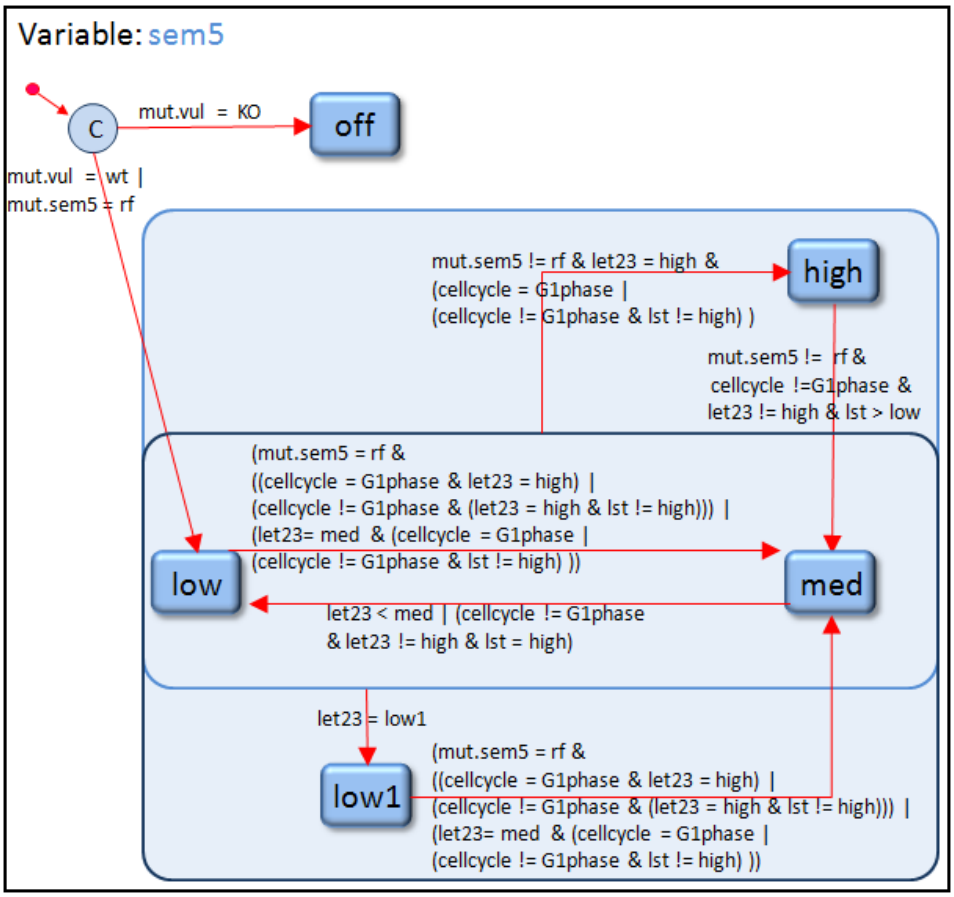

Suppl. Fig. s11. Representation of the state-transitions for the sem5 variable. Blue boxes represent the different possible states of the variable. Red arrows indicate possible transitions. The writing on the arrows indicates the Boolean condition allowing for these transitions. If either of the states in one of the light blue boxes is taken, the transitions originating from the respective box are permitted under the stated conditions in addition to the usual transitions between states. The circled C denotes a condition between two states.

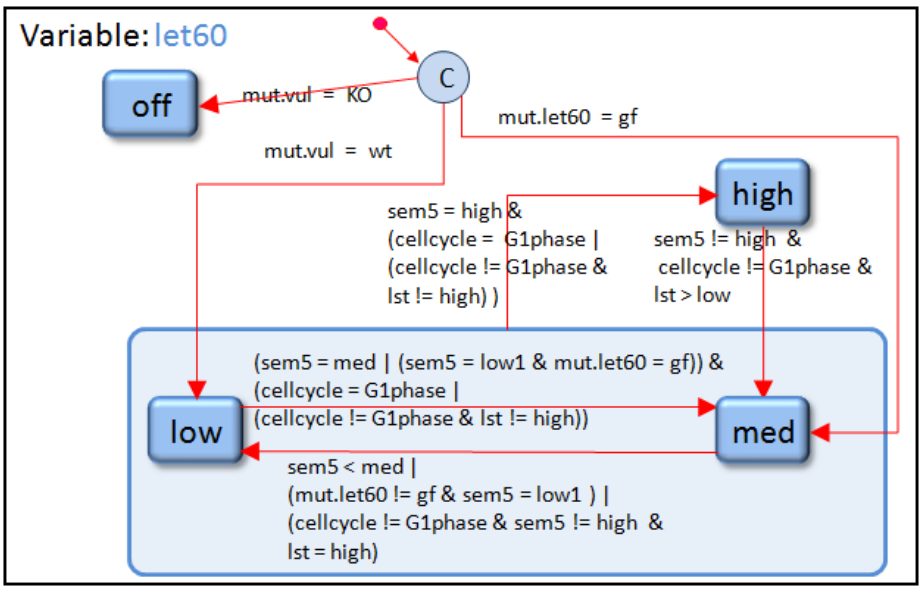

Suppl. Fig. s12. Representation of the state-transitions for the let60 variable. Blue boxes represent the different possible states of the variable. Red arrows indicate possible transitions. The writing on the arrows indicates the Boolean condition allowing for these transitions. If either of the states in the light blue box is taken, the transitions originating from the box are permitted under the stated conditions in addition to the usual transitions between states. The circled C denotes a condition between two states.

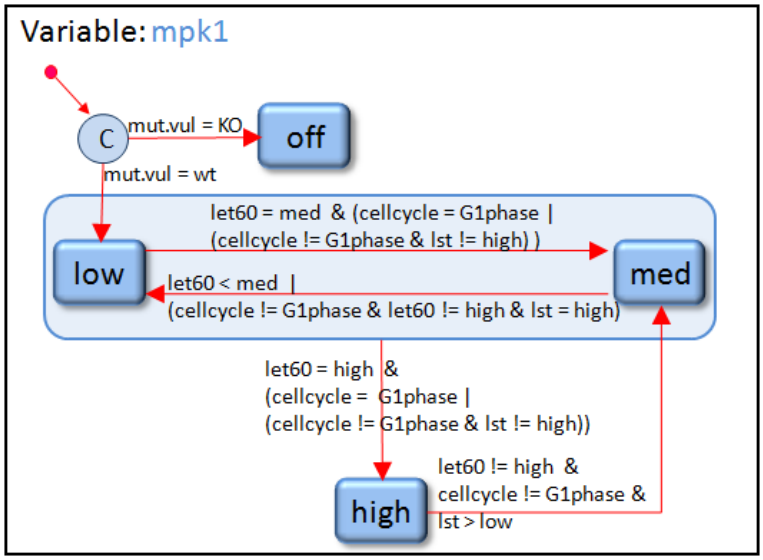

Suppl. Fig. s13. Representation of the state-transitions for the mpk1 variable. Blue boxes represent the different possible states of the variable. Red arrows indicate possible transitions. The writing on the arrows indicates the Boolean condition allowing for these transitions. If either of the states in the light blue box is taken, the transitions originating from the box are permitted under the stated conditions in addition to the usual transitions between states. The circled C denotes a condition between two states.

The EGFR/RAS/MAPK pathway is represented by the variables let23 (corresponding to the EGF receptor), sem5 (corresponding to the Grb2-like adaptor), let60 (corresponding to the RAS GTP-binding protein) and mpk1 (corresponding to the MAP kinase). In our model, we consider mutations resulting in uniform consequences for the whole EGFR/RAS/MAPK pathway and single mutations of components in the pathway that cause a perturbation of the pathway behavior. The wild-type behavior of the pathway is an example for a uniform consequence from setting all of the pathway variables to a wild-type state, i.e. not mutating them. Complete loss of function in at least one of the pathway components (i.e. the variable is set to off) can also be considered as a "uniform mutation" as it causes the pathway downstream of this component to be effectively turned off and, hence, the downstream targets are not activated. Single component mutations permitted in our model are reduced function of sem5 and gain of function in let60. In wild-type conditions all of the variables representing this pathway start at a low level. Upon receiving the inductive signal from the AC let23 changes its level according to the respective VPC's distance to the AC – that is, with a wild-type AC and wild-type lin15, the cell closest to the AC receives a high signal, its neighbors a medium signal and their neighbors a low signal (see Figure s10). An increase in let23 activity can be

counteracted by the *lst* genes and/or by dep1 as indicated in Figure s6. The inductive signal progresses from let23 over sem5 and let60 to mpk1. Figure 2 shows that each of these stages the EGFR/RAS/MAPK pathway can be counteracted by the *lst* genes. A reduced function mutation in the sem5 variable causes a high signal from let23 to be propagated as a medium signal via sem5 (see Figure s11). In contrast, a gain of function mutation in let60 lets the variable start at a medium level (not low as in wt) as shown in Figure s12. The variable will stay at medium level if it receives a medium signal or a signal between low and medium (called low1 in the model) from sem5 that is not counteracted by the *lst* genes. The low1 signal, which progresses from the AC over the EGFR/RAS/MAPK pathway to let60, is only received by P4.p via ISd2 (see paragraph on the AC module). The outer cells, P3.p and P8.p, receive a low signal via ISd3 because they are too far away from the AC. As shown in Figure s13, mpk1 changes according to the level of let60 unless counteracted by lst.

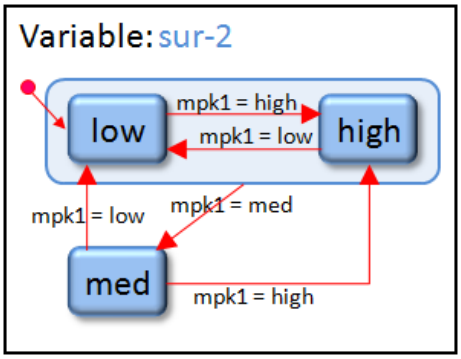

Suppl. Fig. s14. Representation of the state-transitions for the sur2 variable. Blue boxes represent the different possible states of the variable. Red arrows indicate possible transitions. The writing on the arrows indicates the Boolean condition allowing for these transitions. If either of the states in the light blue box is taken, the transitions originating from the box are permitted under the stated conditions in addition to the usual transitions between states.

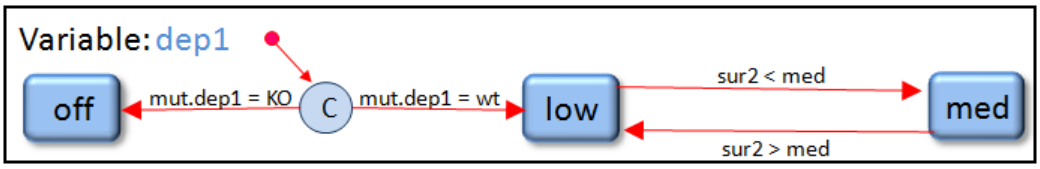

Suppl. Fig. s15. Representation of the state-transitions for the dep1 variable. Blue boxes represent the different possible states of the variable. Red arrows indicate possible transitions. The writing on the arrows indicates the Boolean condition allowing for these transitions. The circled C denotes a condition between two states.

Downstream targets of the EGFR/RAS/MAPK pathway are represented by the variables sur2 and dep1 in our model. The variable sur2 is directly targeted by mpk1 (cf. Figure s6); it starts at a low level and attains the current value of the mpk1 variable in subsequent steps of the execution (see Figure s14). In contrast to most

other variables in the model, dep1 only has the possible values off, low and medium (see Figure s15). A loss of function mutation sets its value to off and, in wild-type conditions, it changes from low to medium if it is not inhibited by a medium or high level of sur2 (for the connectivity, cf. Figure s6). If it is counteracted in this way, dep1 will change from medium to low or stay at a low level.

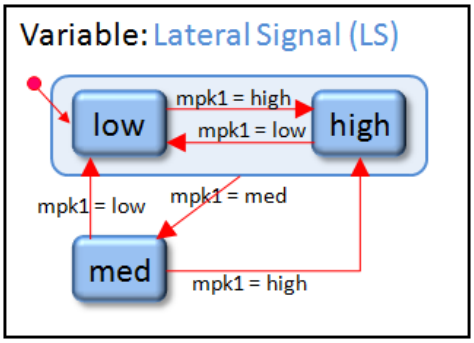

Suppl. Fig. s16. Representation of the state-transitions for the Lateral Signal variable. Blue boxes represent the different possible states of the variable. Red arrows indicate possible transitions. The writing on the arrows indicates the Boolean condition allowing for these transitions. If either of the states in the light blue box is taken, the transitions originating from the box are permitted under the stated conditions in addition to the usual transitions between states.

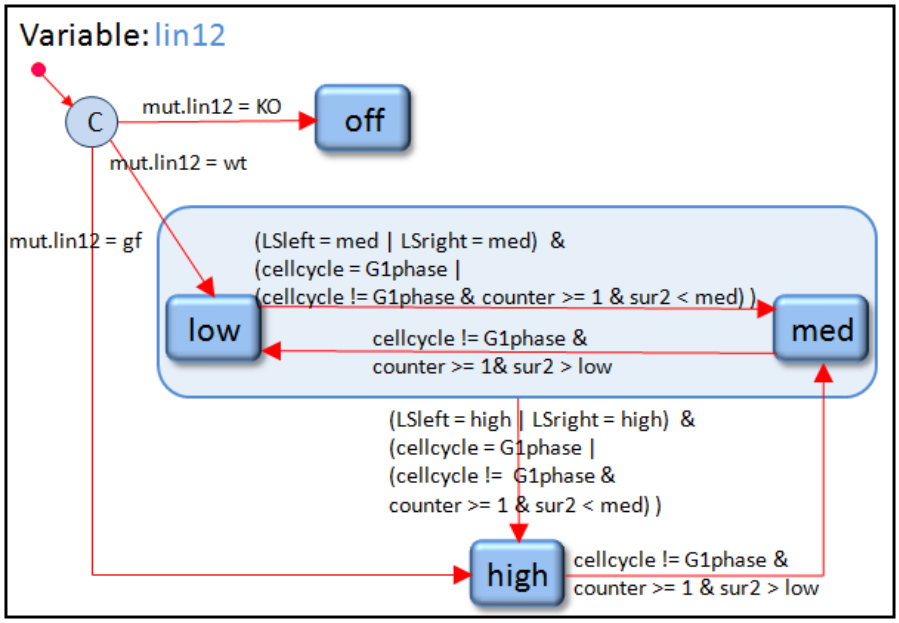

Suppl. Fig. s17. Representation of the state-transitions for the lin12 variable. Blue boxes represent the different possible states of the variable. Red arrows indicate possible transitions. The writing on the arrows indicates the Boolean condition allowing for these transitions. If either of the states in the light blue box is taken, the transitions originating from the box are permitted under the stated conditions in addition to the usual transitions between states. The circled C denotes a condition between two states.

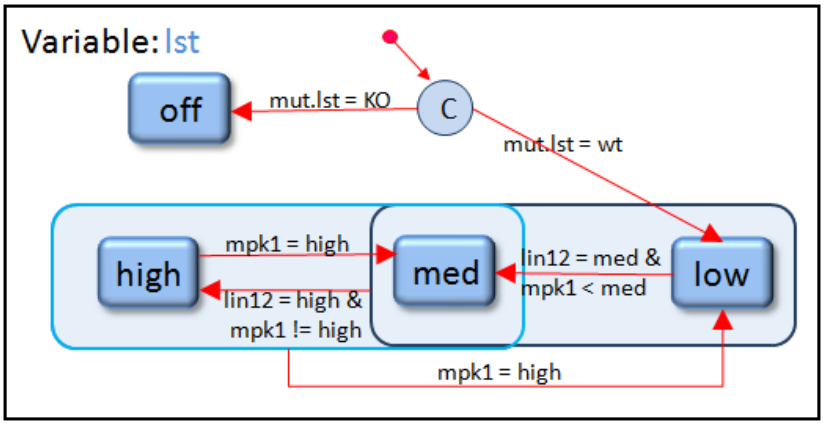

Suppl. Fig. s18. Representation of the state-transitions for the lst variable. Blue boxes represent the different possible states of the variable. Red arrows indicate possible transitions, the writing on the arrows indicates the Boolean condition allowing for these transitions. If either of the states in one of the light blue boxes is taken, the transitions originating from the respective box are permitted under the stated conditions in addition to the usual transitions between states. The circled C denotes a condition between two states.

The level of mpk1 determines the amount of lateral signal that is received by the LIN-12 NOTCH pathway of the neighboring cells (cf. Figure s6) – the variable LS, representing the lateral signal, attains the current value of mpk1 (see Figure s16). In our model, the NOTCH pathway is represented by the variables lin12 (corresponding to the NOTCH receptor) and the variable lst that corresponds to the collective activity state of the *lst* genes *lip-1*, *ark-1*, *dpy-23* and *lst-1* through *lst-4*. In wild-type conditions both variables start at a low level and a loss of function mutation causes the corresponding variable to be set to off (and effectively turn off the pathway). The lin12 variable also allows for a gain of function mutation, which sets the initial value to high as it can be seen in Figure s17. The variable changes according to the lateral signal it receives from both of the neighboring cells, i.e. it attains the higher of these two values unless counteracted by the variable sur2 (connectivity shown in Figure s6). Similarly, the variable lst changes according to the lin12 level unless counteracted by mpk1 (see Figure s18).

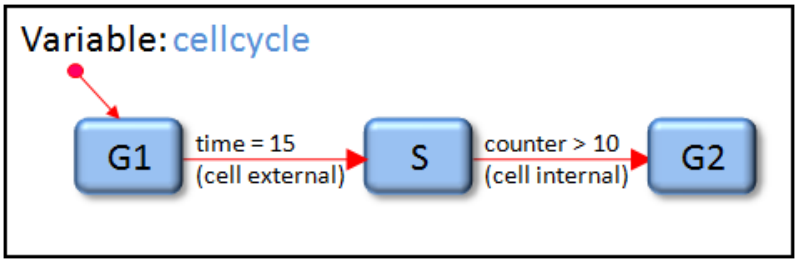

Suppl. Fig. s19. Representation of the state-transitions for the cellcycle variable. Blue boxes represent the different possible states of the variable. Red arrows indicate possible transitions. The necessary timing conditions for the transitions are shown on the arrows.

Our model includes a representation of the cell-cycle as a single variable in each of the VPCs with the possible values G1, S and G2 (corresponding to cell-cycle phases with the respective names). The state diagram of the variable is depicted in Figure s19. We did not include M phase in the cell-cycle variable of our model since it is not relevant for the developmental stage of the worm we look at. The variable starts in G1 and progresses to S in all VPCs simultaneously when an external timer module reaches a threshold time. The progression from S to G2 takes place when a counter internal to each of the VPCs reaches a threshold (i.e. the cells do not have to move to G2 at the same point of the execution).

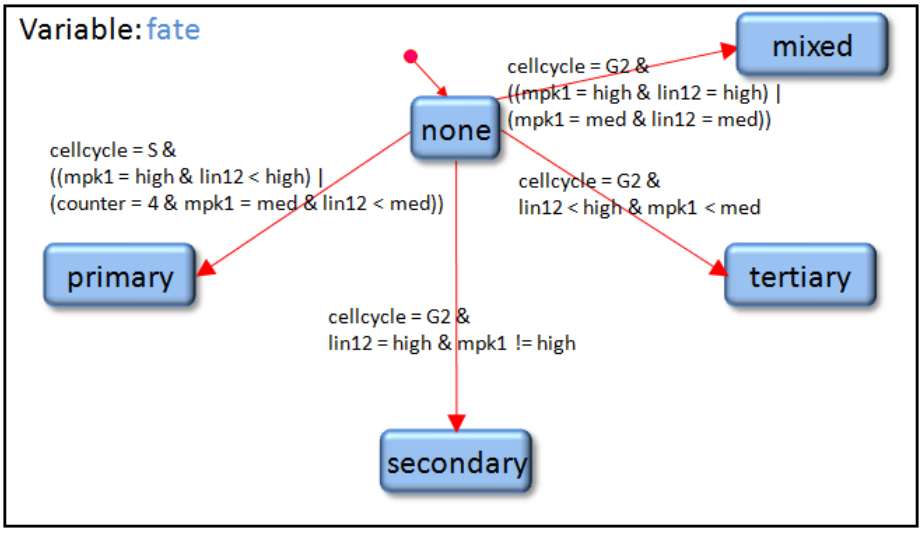

Suppl. Fig. s20. Representation of the state-transitions for the fate variable. Blue boxes represent the different possible states of the variable. Red arrows indicate possible transitions from the none state. The writing on the arrows indicates the Boolean condition allowing for these transitions.

The fate variable in the VPC module starts at the value none and can progress to primary, secondary, tertiary and mixed (see Figure s20). After moving on from none, the fate variable cannot change anymore, i.e. once a cell has obtained a specific fate this will not change again. The different fates are coupled with the cell-cycle as presented in [2]. The fate variable can change from none to primary if at some point in S phase of the cell-cycle mpk1 is higher than lin12. It will attain secondary fate if in G2 phase lin12 is higher than mpk1 or tertiary fate if the variable lin12 has a value below high and the variable mpk1 a value below medium. The value mixed works as a help during model refinement. This value is taken if in G2 phase lin12 and mpk1 are both either at a high or at a medium value at the same time, i.e. if none of the biologically relevant fates are adopted.

Model Analysis

We have analyzed our model using a technique called model checking [3]. The technique allows to formally check all possible executions of the model system against a formal predicate specifying properties of the model that are expected to hold (in our case: specific vulval fate patterns based on genetic perturbations of model variables). Especially in the case of non-deterministic models (as the present one) model checking can significantly speed up the process of testing their consistency with given experimental data. The number of possible executions resulting from one initial state of a non-deterministic model can be very big so that a single simple simulation would not suffice to verify specific properties of a model. Running many simulations (ideally one for each possible scenario) is inevitable in this case. Model checking however explores all possible states and transitions of the given model to test if the specified predicate always holds for the whole model system. If it does not hold in all cases, the algorithm (in our case the NuSMV tool) returns a "counterexample" to the given predicate. A "counterexample" is an execution of the model where some variables violate the predicate at some point of the execution. Looking at this execution step by step enables us to discover what has been inconsistent in the model's definition to correct for the contradiction by refining the model. Note however that the algorithm will always return at most one counterexample (usually the simplest one) even if there have been more executions violating the predicate. Hence, there could be more contradictions than the ones shown in the given execution.
We have used the model checking technique to test if our model reproduces the expected biological behavior for different genetic backgrounds. To this end we formalized the biological data using the genetic perturbations as initial states of the variables in the model (wt, ko, gf, rf) and interpreting the system's behavior as a corresponding fate pattern (suppl. Table 1). The data consist of results from the literature (references given in the last column) and expected values that have not been tested experimentally yet because of general technical difficulties (e.g. larval lethality). We validated our model by checking if predicates representing each of the rows in Table 1 held in all possible executions. The model presented here reproduced all 57 fate patterns from the according genetic perturbations, so we can consider it a valid model of the VPC system.

									Fate pattern						
	AC	lin12	lin15	let60	sem5	dep1	Vul	lst	P3.p	P4.p	P5.p	P6.p	P7.p	P8.p	Reference & Remarks
1	Formed	wt	wt	wt	wt	wt	wt	wt	3	3	2	1	2	3	[4]
2	Formed	wt	wt	wt	wt	wt	wt	ko	3	3	1	1	1	3	[5], [6](by marker expression)
3	Formed	wt	wt	ko	ko	wt	ko	wt	3	3	3	3	3	3	[7]
4	Formed	wt	wt	ko	ko	wt	ko	ko	3	3	3	3	3	3	n.d., only partial Vul(rf) mutants tested
5	Formed	wt	wt	wt	wt	ko	wt	wt	3	3	2	1	2	3	[5]
6	Formed	wt	wt	wt	rf	wt	wt	wt	3	3	3	1	3	3	[5]
7	Formed	wt	wt	gf	wt	wt	wt	wt	3	1	2	1	2	3	[5]
8	Formed	wt	rf	wt	wt	wt	wt	wt	2	1	2	1	2	1	[8]
9	Formed	wt	wt	wt	rf	ko	wt	wt	3	3	3	1	3	3	[5]
10	Formed	wt	wt	gf	wt	ko	wt	wt	2\3	1\2	1\2	1	1\2	1\2	[5]
11	Formed	wt	ko	wt	wt	wt	wt	wt	1\2	1\2	2	1	2	1\2	[7]
12	Formed	wt	ko	wt	wt	wt	wt	ko	1	1	1	1	1	1	[9] (marker expression)
13	Formed	wt	ko	ko	ko	wt	ko	wt	3	3	3	3	3	3	[10], [7] ,[11]
14	Formed	wt	ko	wt	wt	ko	wt	wt	1\2	1\2	1\2	1	1\2	1\2	[5]
15	Formed	wt	ko	ko	ko	wt	ko	ko	3	3	3	3	3	3	n.d.
16	Formed	ko	wt	wt	wt	wt	wt	wt	3	3	1	1	1	3	[7], [12]
17	Formed	ko	wt	wt	wt	wt	wt	ko	3	3	1	1	1	3	Berset & Hajnal, unpublished results
18	Formed	ko	wt	ko	ko	wt	ko	wt	3	3	3	3	3	3	[7](rf Vul mutants)
19	Formed	ko	wt	ko	ko	wt	ko	ko	3	3	3	3	3	3	n.d.
20	Formed	ko	ko	wt	wt	wt	wt	wt	1	1	1	1	1	1	[7]
21	Formed	ko	ko	wt	wt	wt	wt	ko	1	1	1	1	1	1	n.d.
22	Formed	ko	ko	ko	ko	wt	ko	wt	3	3	3	3	3	3	n.d.
23	Formed	ko	ko	ko	ko	wt	ko	ko	3	3	3	3	3	3	n.d.
24	Formed	gf	wt	wt	wt	wt	wt	wt	2	2	2	1	2	2	[7] [lin-12(gf)/lin-12(lf)]
25	Formed	gf	wt	wt	wt	wt	wt	ko	2	2	1	1	1	2	n.d.
26	Formed	gf	wt	ko	ko	wt	ko	wt	2	2	2	2	2	2	[7] [(lin-12(gf)/lin-12(lf) with vul(rf)]
27	Formed	gf	wt	ko	ko	wt	ko	ko	2	2	2	2	2	2	n.d.
28	Formed	gf	ko	wt	wt	wt	wt	wt	1\2	1\2	2	1	2	1\2	[7] [(lin-12(gf)/lin-12(lf)]
29	Formed	gf	ko	wt	wt	wt	wt	ko	1	1	1	1	1	1	n.d
30	Formed	gf	ko	ko	ko	wt	ko	wt	2	2	2	2	2	2	n.d
31	Formed	gf	ko	ko	ko	wt	ko	ko	2	2	2	2	2	2	n.d
32	Ablated	wt	wt	wt	wt	wt	wt	wt	3	3	3	3	3	3	[13]
33	Ablated	wt	wt	wt	wt	wt	wt	ko	3	3	3	3	3	3	[5]
34	Ablated	wt	wt	ko	ko	wt	ko	wt	3	3	3	3	3	3	n.d.
35	Ablated	wt	wt	ko	ko	wt	ko	ko	3	3	3	3	3	3	n.d.
36	Ablated	wt	wt	wt	wt	ko	wt	wt	3	3	3	3	3	3	[5]
37	Ablated	wt	rf	wt	wt	wt	wt	wt	2	1	2	1	2	1	[8]
38	Ablated	wt	ko	wt	wt	wt	wt	wt	1\2	1\2	1\2	1\2	1\2	1\2	[7]
39	Ablated	wt	ko	wt	wt	wt	wt	ko	1	1	1	1	1	1	n.d.
40	Ablated	wt	ko	ko	ko	wt	ko	wt	3	3	3	3	3	3	n.d.
41	Ablated	wt	ko	ko	ko	wt	ko	ko	3	3	3	3	3	3	n.d.
42	Ablated	ko	wt	wt	wt	wt	wt	wt	3	3	3	3	3	3	[7]
43	Ablated	ko	wt	wt	wt	wt	wt	ko	3	3	3	3	3	3	n.d.
44	Ablated	ko	wt	ko	ko	wt	ko	wt	3	3	3	3	3	3	n.d
45	Ablated	ko	wt	ko	ko	wt	ko	ko	3	3	3	3	3	3	n.d.
46	Ablated	ko	ko	wt	wt	wt	wt	wt	1	1	1	1	1	1	[7] (one animal)
47	Ablated	ko	ko	wt	wt	wt	wt	ko	1	1	1	1	1	1	n.d.
48	Ablated	ko	ko	ko	ko	wt	ko	wt	3	3	3	3	3	3	n.d.
49	Ablated	ko	Ko	ko	ko	wt	ko	ko	3	3	3	3	3	3	n.d.
50	Ablated	gf	Wt	wt	wt	wt	wt	wt	2	2	2	2	2	2	[7]
51	Ablated	gf	Wt	wt	wt	wt	wt	ko	2	2	2	2	2	2	[5](for lip-1)
52	Ablated	gf	Wt	ko	ko	wt	ko	wt	2	2	2	2	2	2	[7] (rf mutants), [14]
53	Ablated	gf	Wt	ko	ko	wt	ko	ko	2	2	2	2	2	2	n.d.
54	Ablated	gf	Ko	wt	wt	wt	wt	wt	1\2	1\2	1\2	1\2	1\2	1\2	[7]
55	Ablated	gf	Ko	wt	wt	wt	wt	ko	1	1	1	1	1	1	n.d.
56	Ablated	gf	Ko	ko	ko	wt	ko	wt	2	2	2	2	2	2	n.d.
57	Ablated	gf	Ko	ko	ko	wt	ko	ko	2	2	2	2	2	2	n.d

Suppl. Table 1. Table showing 57 genetic perturbations of components in the VPC model and the respective cell fates of the VPCs with references where applicable. Fates of the different VPCs are color coded; yellow represents tertiary fate, red stands for secondary and blue for primary fate. Purple and orange coloring indicates that the respective cell could have one of two fates (primary/secondary when purple or secondary/tertiary when orange).

Coupling LIN-12 NOTCH degradation to the cell-cycle

Inhibition of lin-12 by sur-2 takes place after the G1 phase of the cell-cycle

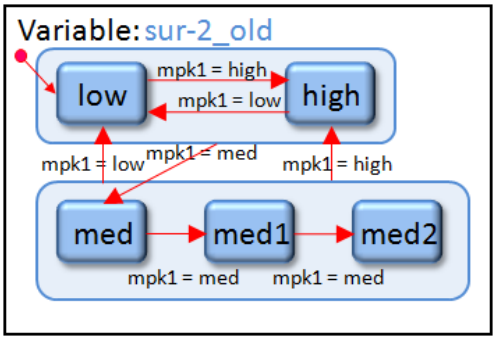

Suppl. Fig. s21. Representation of the state-transitions for the sur2 variable before the introduction of the cell-cycle into the model. Blue boxes represent the different possible states of the variable. Red arrows indicate possible transitions. The writing on the arrows indicates the Boolean condition allowing for these transitions. If either of the states in one of the light blue boxes is taken, the transitions originating from the respective box are permitted under the stated conditions in addition to the usual transitions between states.

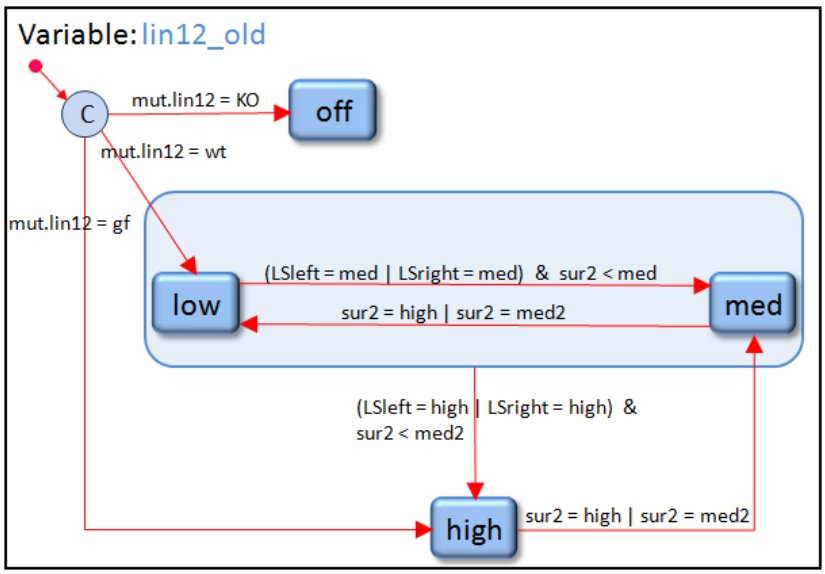

Suppl. Fig. s22. Representation of the state-transitions for the lin12 variable before the introduction of the cell-cycle into the model. Blue boxes represent the different possible states of the variable. Red arrows indicate possible transitions. The writing on the arrows indicates the Boolean condition allowing

for these transitions. If either of the states in the light blue box is taken, the transitions originating from the box are permitted under the stated conditions in addition to the usual transitions between states. The circled C denotes a condition between two states.

Before introducing the cell-cycle into our model, an artificial delay in the variable sur2 was necessary to reproduce the proper behavior of lin12 and hence the correct fate patterns shown in Table 1. This delay was realized such that sur2 had to stay in a medium state for two steps of the execution before being able to inhibit lin12 (see Figure s21 and Figure s22). If the level of sur2 was high, inhibition of lin12 was allowed straight away. With the introduction of the cell-cycle, we removed this delay and coupled the inhibition of lin12 to the state of the cell-cycle variable (see Figure s14 and Figure s17). In a first *in silico* experiment, we allowed for the inhibition of lin12 only to happen during G1 phase. This configuration of the model produced several counterexamples to the experimental data shown in Table 1. We further tested a model where lin12 inhibition was forbidden in G1 phase but allowed in the S or G2 phase, which is the configuration of the model presented here. Model checking has shown that this configuration is consistent with all of the experimental results and we can thus predict that *lin-12* is downregulated after G1 phase.

Supplementary References

1. Cimatti A, Clarke E, Giunchiglia E, et al. NuSMV 2: An OpenSource Tool for Symbolic Model Checking. Berlin, Heidelberg: Springer Berlin Heidelberg; 2002, 2404:241-268.

2. Ambros V: Cell-cycle-dependent sequencing of cell fate decisions in Caenorhabditis elegans vulva precursor cells. Development 1999, 126:1947-1956.

3. Clarke EM, Grumberg O, Peled D: Model checking. MIT Press; 1999:314.

4. Sulston JE, Horvitz HR: Post-embryonic cell lineages of the nematode, Caenorhabditis elegans. Developmental Biology 1977, 56:110-156.

5. Berset TA, Hoier EF, Hajnal A: The C. elegans homolog of the mammalian tumor suppressor Dep-1/Scc1 inhibits EGFR signaling to regulate binary cell fate decisions. Genes & development 2005, 19:1328-40.

6. Yoo AS, Bais C, Greenwald I: Crosstalk between the EGFR and LIN-12/Notch pathways in C. elegans vulval development. Science (New York, N.Y.) 2004, 303:663-6.

7. Sternberg PW, Horvitz HR: The combined action of two intercellular signaling pathways specifies three cell fates during vulval induction in C. elegans. Cell 1989, 58:679-693.

8. Dutt A, Canevascini S, Froehli-Hoier E, Hajnal A: EGF signal propagation during C. elegans vulval development mediated by ROM-1 rhomboid. PLoS biology 2004, 2:e334.

9. Berset T, Hoier EF, Battu G, Canevascini S, Hajnal a: Notch inhibition of RAS signaling through MAP kinase phosphatase LIP-1 during C. elegans vulval development. Science (New York, N.Y.) 2001, 291:1055-8.

10. Ferguson EL, Sternberg PW, Horvitz HR: A genetic pathway for the specification of the vulval cell lineages of Caenorhabditis elegans. Nature 1987, 326:259-67.

11. Cui M, Kim EB, Han M: Diverse chromatin remodeling genes antagonize the Rb-involved SynMuv pathways in C. elegans. PLoS genetics 2006, 2:e74.

12. Greenwald IS, Sternberg PW, Robert Horvitz H: The lin-12 locus specifies cell fates in Caenorhabditis elegans. Cell 1983, 34:435-444.

13. Kimble J: Alterations in cell lineage following laser ablation of cells in the somatic gonad of Caenorhabditis elegans. Developmental Biology 1981, 87:286-300.

14. Han M, Aroian RV, Sternberg PW: The let-60 Locus Controls the Switch Between Vulval and Nonvulval Cell Fates in Caenorhabditis elegans. Genetics 1990, 126:899-913.

Supplementary Table 2

Donor vector	Entry clone	primer
pDONR P4-P1r	pIN8 contains promoter of *bar-1*	OIN88 ATAGAAAAGTTGCTTAGCAAAGCCGTGTCAAAACCC OIN89 TGTACAAACTTGTAGGTTCGGATCCAGGTCCATCCC
pDONR P2R-P3	pCH17 contains 3′-UTR of *unc-54*	OCH54 TGTACAAAGTGGGTGCCTCTGACTTCTAAGTCC OCH55 ATAATAAAGTTGGGAAACAGTTATGTTTGGTATATTGGG
pCFJ150	pSN16 containing NICD::GFP (cDNA of GS3201 was used as template.)	OSN147 AAAAAGCAGGCTATGACAAGGAAACGTCGAATGATCAACG OSN138 AGAAAGCTGGGTTCAAAAATAATGAGCTGGTTCGGAG
	pSN26 containing YFP	OCH46 AAAAAGCAGGCTCTATGACTGCTCCAAAGAAGAAGCG OCH47 AGAAAGCTGGGTTGACACCAGACAAGTTGGTAATG
	pSN27 containing NICD::GFPΔCT	OSN147 AAAAAGCAGGCTATGACAAGGAAACGTCGAATGATCAACG OSN230 GGGGACCACTTTGTACAAGAAAGCTGGGTTCATGAGTCTCGACC
	pSN29 containing NICD::GFPΔNT	OSN255 GGGGACAAGTTTGTACAAAAAAGCAGGCTATGAGTAAAGGAGAAGAACTTTTC OCH138 AGAAAGCTGGGTTCAAAAATAATGAGCTGGTTCGGAG
	pSN34 containing NICD::GFPΔANK	Using Fusion PCR a construct that misses the ankrin repeats was made with the following primers. This construct was cloned using gateway system into pCFJ150. OSN147 AAAAAGCAGGCTATGACAAGGAAACGTCGAATGATCAACG OSN250 CCAGTGAAAAGTTCTTCTCCTTTACTCATATTCCCGTATCCTTGAGGATTTGG Left GFP ATGAGTAAAGGAGAAGAACTTTTCACTGG OSN138 AGAAAGCTGGGTTCAAAAATAATGAGCTGGTTCGGAG

Suppl. Table 2. Plasmid constructs and primers used in this study. The different NICD::GFP constructs were cloned into pDONR221. Together with the pIN8 and pCH17 they were inserted via the gateway method into the pCFJ150 MosSci vector.